35th International Conference on Lightning Protection
XVI International Symposium on Lightning Protection
20th to 26th September 2021 - Sri Lanka
ICLP-SIPDA SRI LANKA 2021

Säntis Lightning Research Facility Instrumentation

A. Sunjerga, A. Mostajabi, M. Paolone, F. Rachidi*
EMC Laboratory
EPFL
Lausanne, Switzerland
*farhad.rachidi@epfl.ch

M. Azadifar, A. Rubinstein, M. Rubinstein
Institute for Information and Communication Technologies
University of Applied Sciences of Western Switzerland
Yverdon-les-Bains, Switzerland

C. Romero
Armasuisse
Bern, Switzerland

D. Pavanello
Institute of Sustainable Energy
University of Applied Sciences of Western Switzerland,
Sion, Switzerland

P. Hettiarachchi, V. Cooray
Department of Engineering Sciences
Uppsala University
Uppsala, Sweden

D. Smith
Institute for Particle Physics and Department of Physics,
University of California,
Santa Cruz, California

***Abstract*— The Säntis Tower was instrumented in May 2010 to measure currents of lightning discharges striking the tower. Since then the system has been recurrently updated and expanded. Currently, data associated with lightning strikes to the tower are collected at five different sites. The facility is equipped with a current measurement system, three electric field antennas, an electrostatic field mill, two x-rays sensors, a high-speed camera and four full HD cameras. This paper presents the latest measurement configuration at the facility.**

Keywords-lightning,measurements, Säntis Tower, upgrade, current, camera, high-speed, X-rays

I. INTRODUCTION

The Säntis Tower is a 124-m-tall tower sitting at the top of the 2502-m tall Säntis Mountain (see Fig. 1). The Säntis Mountain is located in the northeast of Switzerland in the Appenzell region (47°14'57" N, 9°20'32" E). The tower is struck by lightning about 100 times per year.

The tower has been instrumented for lightning current measurements since May 2010 [1-3]. In 2014, an electric field station was installed at about 15 km away from the tower [4]. Also, since 2014, the trigger has been sent using TCP/IP over the Internet to the 380 km distant electric field sensor location in Neudorf, northern Austria, operated by ALDIS. More details on the Neudorf station can be found in [5,6]. Here, we present for the first time new measurement stations installed since then.

This paper presents a summary of the measurement systems deployed at the tower and its vicinity. The paper is organized as follows. Section II presents an overview of all the measurement sites and sensors. Sections III to VI present in detail recent upgrades and newly installed equipment.

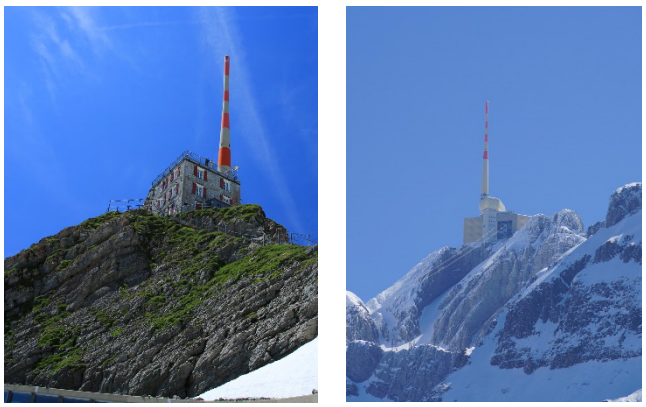

a.) b.)

Fig. 1. Säntis Tower at the top of the 2502-m tall Säntis Mountain. (a) Summer, (b) Winter.

I. OVERVIEW OF THE SÄNTIS RESEARCH FACILITY

A. Measurement Sites

Fig. 2 presents a simplified sketch of the seven measurement sites belonging to the Säntis research facility. The measurement systems deployed in each site are briefly described in what follows.

978-1-6654-2346-5/21/$31.00 ©2021 IEEE

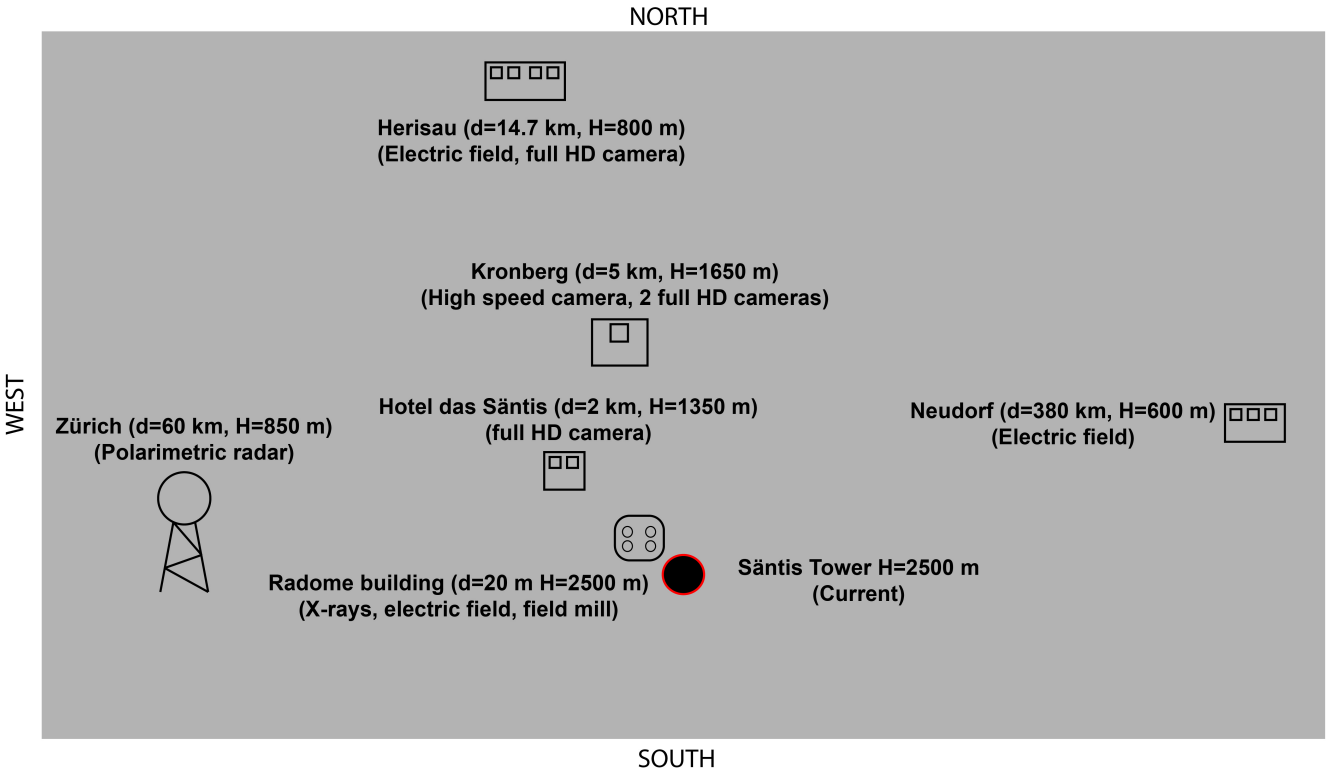

Fig. 2. Simplified sketch of different observational sites and measuring sensors including their distance to the tower and their geographical altitude. Not to scale.

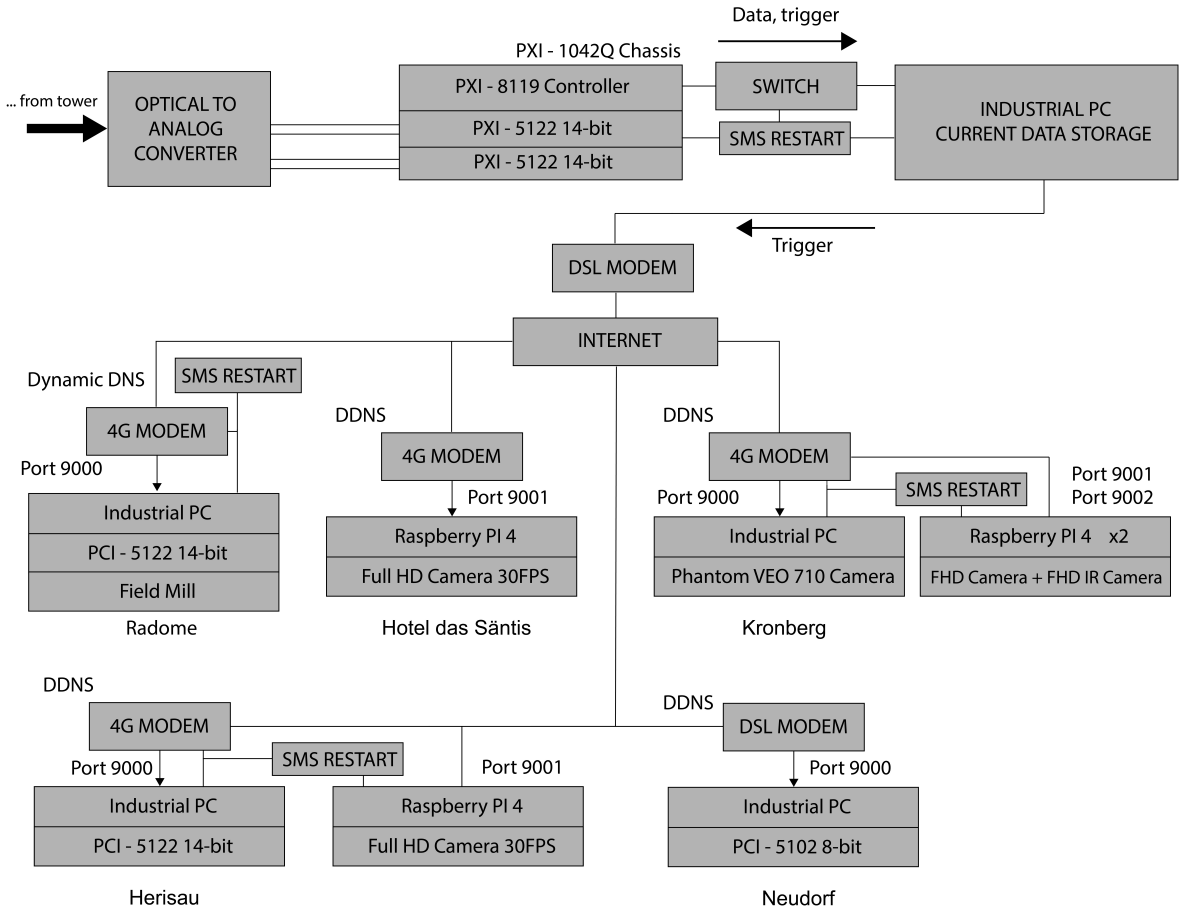

Fig. 3. Simplified graph of the measuring system. The TCP trigger is sent from the tower to all other trigger-based sites.

1. The Säntis Tower (2502 m ASL). Lightning current and its time derivative are measured at two different heights (24 m and 82 m above ground level), using at each location a Rogowski coil and a B-dot sensor. The measurement systems on the tower are thoroughly described in [1-3].
2. Radome (2500 m ASL). The radome is located about 20 m away from the tower (see Fig. 4). At this location, we have installed a fast electric field antenna, an electrostatic field mill, and two x-rays sensors, belonging to our partners from Uppsala University and the University of California at Santa Cruz.
3. Säntis - Das Hotel (1400 m ASL). Located about 2 km away from the tower on the slope of Mount Säntis, this station is equipped with a full HD camera.
4. Mount Kronberg (1663 m ASL) is about 5 km away from the tower. At this location, a high-speed video camera and two FHD cameras are installed. One of the FHD cameras operates in the visible spectrum, while the other one works in the infra-red (IR) spectrum.
5. Herisau (800 m ASL). This site is located at a distance of 14.7 km of the tower. A fast E-field antenna is installed on the top of a building belonging to the Huber+Suhner company.
6. Neudorf (600 m ASL). This station, operated by ALDIS, is located in Neudorf, northern Austria, 380 km away from the tower. The station is equipped with a fast E-field antenna.
7. Albis radar located near the city of Zurich, 60 km east from the Säntis area [7,8].

It is worth noting that the Säntis Tower area is also covered by the EUCLID lightning location network [9]. The Säntis area was also covered by a lightning mapping array (LMA) belonging to the Polytechnic University of Catalunya during an experimental campaign organized in the Summer of 2017 [8]. In addition, during the Summer of 2019 an interferometer belonging to the New Mexico Tech was installed near the Säntis Hotel and, as of the writing of this paper, it will be installed in the Summer of 2020.

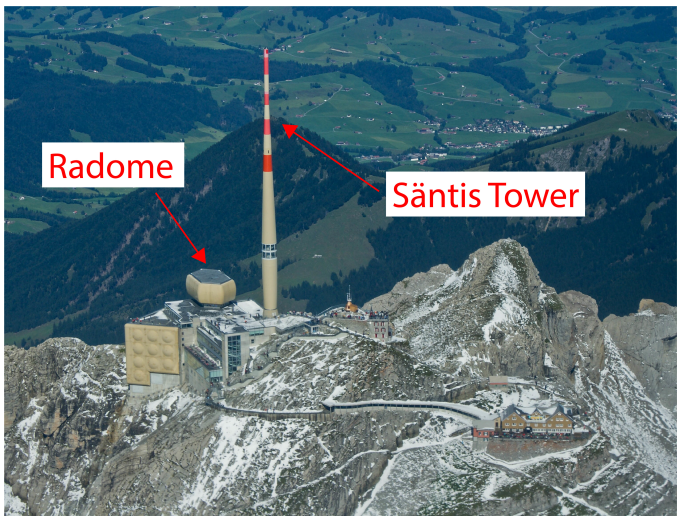

Fig. 4. Location of radome next to the tower.

At each measuring site, every relevant equipment is connected to the modem and has a fixed private local IP non-visible to the rest of the Internet. The modem is configured in such a way that one free port is allocated for each device with their static IP address. For example, in the case of the Kronberg site, three triggers will be sent from the current measuring site using TCP/IP to the URL belonging to the modem installed at this site but using different ports (e.g., 9000, 9001, 9002), one for each camera. This URL is pointing to the IP address of the modem and, in case of a change of IP address of the modem, this URL will be updated to point to the new IP address. This is achieved with the DDNS method and a client installed on one of the PCs connected to the modem. The modem is configured in such a way that the ports are forwarded to the static local IP address of each connected device.

Once each of the devices receives the data, they immediately trigger the corresponding measuring equipment. They all operate with appropriate pre-trigger times with data stored in the buffer. After receiving the trigger, they will continue to work for a time defined by the post-trigger window during which the data are recorded. Since most of the stations communicate over the 4G network, the latency is not always constant. However, most of the time the delay is no longer than 100 ms.

Since the location of the Säntis Tower is more than 200 km away from our laboratory and physical access to the tower and the radome is possible only three days per month, the remote control is of high importance. The remote control commands are transmitted over the Internet, with the inherent risk that a power failure and an interruption in the Internet access can cause disconnection. When the system at the tower is shut down (due to power outages or to voluntary power cycling operations at the tower), or when it loses its Internet connection, it is not able to send trigger signals to the other measuring sites. This can cause the loss of valuable data. In order to mitigate the problem of loss of Internet connection, we have added redundancy to the remote-control system using a GSM receiver. This system, shown in Fig. 5, can be controlled by sending codes in SMS messages to remotely power-cycle either one of the local PCs or the Internet modem since we have determined through experience that this solves most of the connection loss problems. The system is installed at four different locations as shown in Fig. 3.

In the following section, we will report on recent updates at the measuring stations. Details about the current measurement system as well as the remote electric field station in Neudorf can be found in previous literature [1-6]. The instrumentation in the three new stations (radome, Hotel and Kronberg) have not been reported elsewhere. We will give a summary of the instrumentation for each of these sites. Even though some information about the Herisau station has been already provided in [4], we will present here the latest upgrades made to that system.

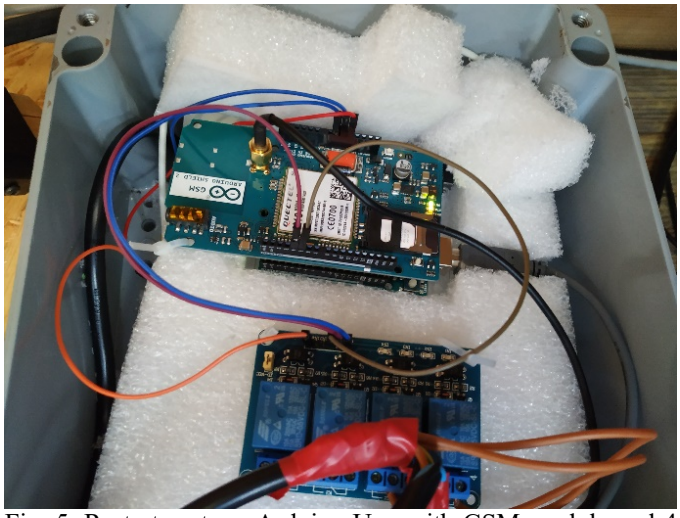

Fig. 5. Restart system. Arduino Uno with GSM module and 4 channel relays.

II. RADOME

This station is located 20 m away from the tower (see Fig. 4). It is equipped with an industrial PC with a two-channel PCI digitizer. One channel of the digitizer is connected to a fast E-field antenna while the second is connected to one of the X-ray sensors. The sampling rate is set to 50 MS/s with a pre-trigger delay of 1.2 s. Each record is 2.4 s long. The field mill is connected via USB to the same PC and the data are recorded in continuous mode. A Garmin GPS 18x LVC is connected to the serial port of the industrial computer and provides a time accuracy of several microseconds.

A commercial microphone is also installed and connected to the PC via USB cable. It is operated via LabView and provides recording for a duration of 100 s. The data will be saved only when a trigger is received.

A. Fast antenna

A commercial Thales (former Thomson CSF) Mélopée electric field sensor with a frequency range of 1 kHz to 150 MHz was installed during the Summer of 2018 (see Fig. 6). The output of this antenna is connected to the first channel of the digitizer. More information about the system can be found in [4]. Note that this antenna was initially located in Herisau and it was moved to the radome site in 2018. The antenna in Herisau was replaced with a flat plate antenna (see Section VI).

B. X-ray sensors

In July 2019, an X-ray sensor (see Fig. 7) from Uppsala University [11,12] was installed in the radome. In order to mitigate the coupling and interference of strong lightning electromagnetic fields to the measuring system, a battery power supply was installed in the metallic box containing the X-ray measuring device. This system consists of two batteries and a microcontroller that manages the charging of the batteries in such a way that the charging alternates between the two. While one battery is being charged, the other is used as the power supply, so that the system is never connected galvanically to the 230 V grid, preventing any conducted interference from reaching the equipment. Furthermore, the 230 V power supply is provided from an insulation transformer to further reduce noise in cables and possible field coupling. To further reduce the noise, the analog output of the X-ray sensor is relayed to the second channel of the digitizer via a fiberoptic link.

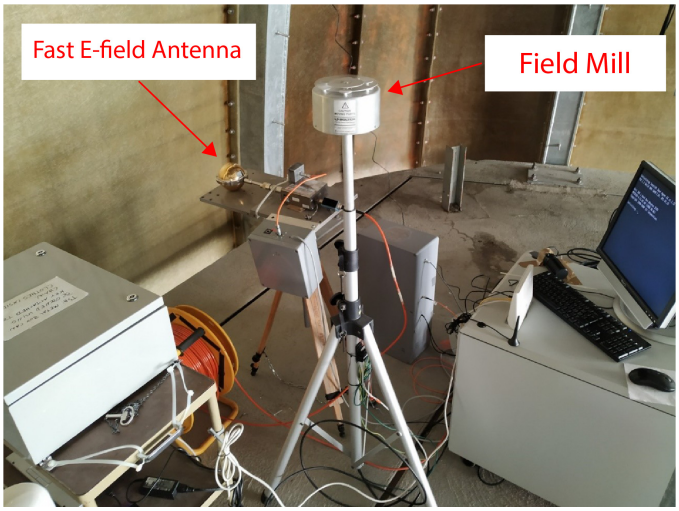

Fig. 6. Fast E-field antenna and field mill.

Another X-ray sensor belonging to the University of California, Santa Cruz (see Fig. 8) was also installed in July 2019. The detector is a 5-inch (diameter) x 5-inch (length) cylinder of BC-408 plastic mounted to a 5-inch PMT (photomultiplier tube). The PMT is negatively biased by ~850 Volts. The detector output is connected to a Bridgeport Instrument eMorpho MCA (Multi-Channel Analyzer) that uses a time-tagged event mode to record the integrated pulse area (with 16-bit resolution) and the arrival time (with 32-bit/12.5-ns resolution) of the detector output. This amounts to a 80-MHz sampling speed. The combination of the nanosecond decay time of the BC-408 and the sampling speed of the MCA is needed to record the high flux and sub-millisecond arrival times of TGF photons. In addition to the detector chain, there is also a GPS unit where a pulse-per-second signal is fed into the MCA's FPGA and incorporated into the data stream as a flagged event. This allows for a precise relative timing and low data usage since the periods without events are not saved, so the device can operate in continuous mode. This device is connected to a second computer on which the data are saved.

C. Field Mill

To measure the electrostatic field, an EFM-100 field mill has been installed in the same location since 15 July, 2016, as shown in Fig. 6. The field mill is connected via USB to the industrial PC and the data are recorded in continuous mode.

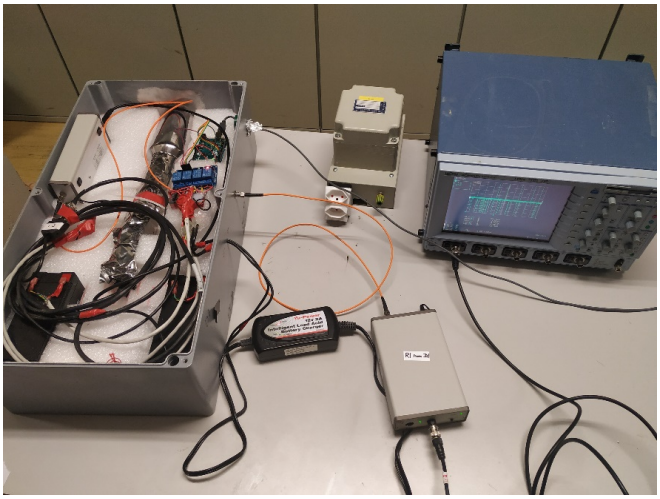

Fig. 7. X-ray sensor from Uppsala University

Fig. 8. X-ray sensor from the University of California, Santa Cruz working in the continuous mode.

III. Hotel das Santis

In Spring 2020, a FHD camera was installed in the hotel located about 2 km of air distance away from the tower and 1150 m below the ASL of top of the mountain. A Raspberry PI 4 with a Camera Module v2 was used for this purpose. The camera has an optical size of 1/4" and a focal ratio equal to 2.0. It can operate in Full HD resolution with 30 FPS and can record images of 4K resolution. Currently the camera is set to an ISO equal to 100 and to record Full HD videos with 30 FPS.

Each Raspberry PI is equipped with a 32 GB SD card and it is connected to the Internet. The main code is written in Python and it consists of two threads. The first is waiting for the trigger over TCP/IP on the chosen port. The second is constantly recording the videos for a duration of 60 seconds. If the trigger is received, the video is saved. Otherwise, the video is deleted. Remote access of the raspberry PI is possible over the Internet.

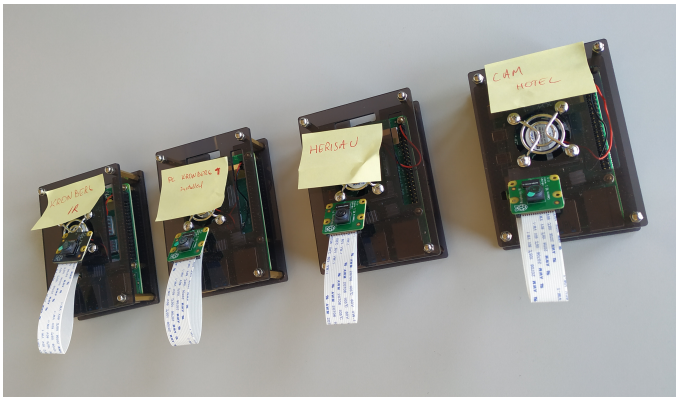

Fig. 9. Four Raspberry PI 4 4G with the camera ready to be installed at three different sites.

IV. Kronberg

A Phantom VEO 710L high-speed video camera is installed at this location. A view of the Säntis Tower from the camera is shown in Fig. 10. The camera can record up to 1,000,000 FPS at its lowest resolution of 8 x 8 pixels. To have a wider view of 512 x 512 pixels, the number of frames per second needs to be reduced to 10,000. These pixels are distributed over a view of about 2 km by 2 km. The camera records during a 3-second time window with a pre-trigger delay of 1.5 s. A GPS time stamp is provided with an Acutime 360 Multi-GNSS Smart Antenna and the synchronization error is within 15 nanoseconds.

Additionally, two FHD cameras as described in Section IV are installed at this location. The first camera works in the visible spectrum and the second on operates in infra-red.

Fig. 10. High speed Phantom VEO 710L camera installed at the top of the Kronberg mountain.

V. Herisau

A flat plate antenna is installed in this location since 2017 and it has been updated several times since then. It has a two-battery system to ensure a noise-free power source since the charging and use of the batteries alternates to avoid having a galvanic connection to the mains as in the case of the X-ray sensor (Section III). An industrial computer with a two-channel digitizer is installed at the station. Integrator is located next to the antenna. Terahertz Technologies LTX-5515 analog to

digital optical link was used to transfer the analog signal to the input of digitizer. The integrator output transferred by optical link and back converted to the analog signal is connected to the first channel of digitizer that can measure voltages from -5 V to 5 V with a 14-bit resolution. The time constant of the antenna is 8 ms and it can measure electric fields in the range from -200 V/m to 200 V/m.

The digitizer is set to a sampling rate of 10 MS/s with a time window of 6 s and a pre-trigger delay of 3 s. The second channel of the digitizer is connected to the pulse per second output of a Garmin GPS 18x LVC unit. This provides a time accuracy of about a microsecond. This site is also equipped with one FHD camera with the same specifications described in Section IV.

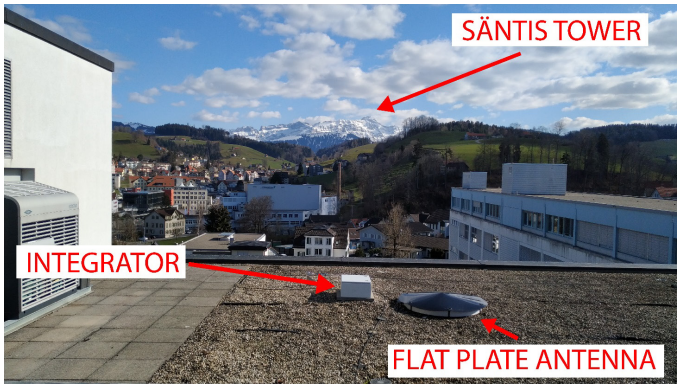

Fig. 11. Flat plate antenna installed at the Herisau site. The antenna is covered with a dielectric for precipitation protection.

VI. Conclusion

In this paper, we presented the measurement system deployed at the Säntis research facility, as well as its recent upgrades. Three new sites in the vicinity of the tower have been equipped with different sensors such a high-speed camera, four FHD cameras, two fast electric field antennas, an electric field mill and two X-rays sensors. The trigger signal is being sent to all stations from the current measurement system over the Internet. Each site can be accessed and controlled remotely. Broadband measurements can help us in future to better understand processes involved in upward lightning.

Acknowledgment

This work was supported in part by the Swiss National Science Foundation (Project No. 200020_175594) and the European Union's Horizon 2020 research and innovation program under grant agreement No 737033-LLR.

References

[1] C. Romero, “Measurement of Lightning Currents Using a Combination of Rogowski Coils and B-Dot Sensors,” Journal of Lightning Research, vol. 4, no. 1, pp. 71–77, Jul. 2012

[2] C. Romero et al., “A system for the measurements of lightning currents at the Säntis Tower,” Electric Power Systems Research, vol. 82, no. 1, pp. 34–43, Jan. 2012, doi: 10.1016/j.epsr.2011.08.011.

[3] Azadifar .M, M. Paolone, D. Pavanello, F. Rachidi, C. Romero, and M. Rubinstein (2014), "An Update on the Instrumentation of the Säntis Tower in Switzerland for Lightning Current Measurements and Obtained Results," in CIGRE International Colloquium on Lightning and Power

[4] D. Li et al., “On Lightning Electromagnetic Field Propagation Along an Irregular Terrain,” IEEE Transactions on Electromagnetic Compatibility, vol. 58, no. 1, pp. 161–171, Feb. 2016, doi: 10.1109/temc.2015.2483018.

[5] Azadifar, M., Li, D., Rachidi, F., Rubinstein, M., Diendorfer, G., Schulz, W., Pichler, H., Rakov, V. A., Paolone, M., & Pavanello, D. (2017). Analysis of lightning-ionosphere interaction using simultaneous records of source current and 380 km distant electric field. Journal of Atmospheric and Solar-Terrestrial Physics, 159, 48–56. https://doi.org/10.1016/j.jastp.2017.05.010

[6] Pichler, H., Diendorfer, G., & Mair, M. (2010). Some Parameters of Correlated Current and Radiated Field Pulses from Lightning to the Gaisberg Tower. IEEJ Transactions on Electrical and Electronic Engineering, 5(1), 8–13. https://doi.org/10.1002/tee.20486

[7] N. Pineda et al., “Meteorological Aspects of Self‐Initiated Upward Lightning at the Säntis Tower (Switzerland),” Journal of Geophysical Research: Atmospheres, vol. 124, no. 24, pp. 14162‐14183, Dec. 2019.

[8] J. Figueras i Ventura et al., “Analysis of the lightning production of convective cells,” Atmospheric Measurement Techniques, vol. 12, no. 10, pp. 5573–5591, Oct. 2019.

[9] W. Schulz, G. Diendorfer, S. Pedeboy, and D. R. Poelman, “The European lightning location system EUCLID – Part 1: Performance analysis and validation,” Natural Hazards and Earth System Sciences, vol. 16, no. 2, pp. 595–605, Mar. 2016, doi: 10.5194/nhess-16-595-2016

[10] A. Sunjerga et al., “LMA observations of upward lightning flashes at the Säntis Tower initiated by nearby lightning activity,” Electric Power Systems Research, vol. 181, p. 106067, Apr. 2020.

[11] P. Hettiarachchi, V. Cooray, G. Diendorfer, H. Pichler, J. Dwyer, and M. Rahman, “X-ray Observations at Gaisberg Tower,” Atmosphere, vol. 9, no. 1, p. 20, Jan. 2018, doi: 10.3390/atmos9010020.

[12] P. Hettiarachchi, M. Rahman, V. Cooray, and J. Dwyer, “X-rays from negative laboratory sparks in air: Influence of the anode geometry,” Journal of Atmospheric and Solar-Terrestrial Physics, vol. 154, pp. 190–194, Feb. 2017.